THE JOURNAL OF BIOLOGICAL CHEMISTRY
Vol. 278, No. 44, Issue of October 31, pp. 43508–43515, 2003
Printed in U.S.A.

Molecular Basis of Vitamin E Action

TOCOTRIENOL MODULATES 12-LIPOXYGENASE, A KEY MEDIATOR OF GLUTAMATE-INDUCED NEURODEGENERATION*[S]

Received for publication, July 2, 2003, and in revised form, August 12, 2003
Published, JBC Papers in Press, August 13, 2003, DOI 10.1074/jbc.M307075200

Savita Khanna‡, Sashwati Roy‡, Hoon Ryu§, Praveen Bahadduri¶, Peter W. Swaan¶, Rajiv R. Ratan§, and Chandan K. Sen‡‖

From the ‡Laboratory of Molecular Medicine, Department of Surgery, and the ¶Bioinformatics and Computational Biology Core Laboratory, Dorothy M. Davis Heart and Lung Research Institute, The Ohio State University Medical Center, Columbus, Ohio 43210 and the §Department of Neurology, Harvard Medical School, and the Beth Israel Deaconess Medical Center, Boston, Massachusetts 02115

Vitamin E is a generic term for tocopherols and tocotrienols. This work is based on our striking evidence that, in neuronal cells, nanomolar concentrations of α-tocotrienol, but not α-tocopherol, block glutamate-induced death by suppressing early activation of c-Src kinase (Sen, C. K., Khanna, S., Roy, S., and Packer, L. (2000) *J. Biol. Chem.* 275, 13049–13055). This study on HT4 and immature primary cortical neurons suggests a central role of 12-lipoxygenase (12-LOX) in executing glutamate-induced neurodegeneration. BL15, an inhibitor of 12-LOX, prevented glutamate-induced neurotoxicity. Moreover, neurons isolated from 12-LOX-deficient mice were observed to be resistant to glutamate-induced death. In the presence of nanomolar α-tocotrienol, neurons were resistant to glutamate-, homocysteine-, and L-buthionine sulfoximine-induced toxicity. Long-term time-lapse imaging studies revealed that neurons and their axo-dendritic network are fairly motile under standard culture conditions. Such motility was arrested in response to glutamate challenge. Tocotrienol-treated primary neurons maintained healthy growth and motility even in the presence of excess glutamate. The study of 12-LOX activity and metabolism revealed that this key mediator of glutamate-induced neurodegeneration is subject to control by the nutrient α-tocotrienol. *In silico* docking studies indicated that α-tocotrienol may hinder the access of arachidonic acid to the catalytic site of 12-LOX by binding to the opening of a solvent cavity close to the active site. These findings lend further support to α-tocotrienol as a potent neuroprotective form of vitamin E.

Vitamin E is a generic term for tocopherols and tocotrienols, which qualitatively exhibit the biological activity of α-tocopherol (1). Compared with tocopherols, tocotrienols have been poorly studied (2, 3). Tocotrienols differ from tocopherols by possessing a farnesyl (isoprenoid) rather than a saturated phytyl side chain. Dietary tocotrienols become incorporated into circulating human lipoproteins, where they react with peroxyl radicals as efficiently as the corresponding tocopherol isomers (4, 5). Indeed, tocotrienol supplementation beneficially influences the course of carotid atherosclerosis in humans (6). Following supplementation to humans, the level of α-tocotrienol in the plasma has been estimated to be 1 μM (7). At concentrations of 25–50 μM, α-tocopherol is known to regulate signal transduction pathways by mechanisms that are independent of its antioxidant properties (8, 9). Micromolar amounts of tocotrienol, but not tocopherol, have been shown to suppress the activity of hydroxy-3-methylglutaryl-coenzyme A reductase (10, 11). The unsaturated side chain of tocotrienol allows for more efficient penetration into tissues that have saturated fatty layers such as the brain and liver (12).

Glutamate toxicity is a major contributor to pathological cell death within the nervous system. There are two forms of glutamate toxicity: receptor-initiated excitotoxicity (13) and non-receptor-mediated toxicity (14). One established model (15, 16) used to study oxidative stress-related neuronal death is to inhibit cystine uptake by exposing cells to high levels of glutamate (17). Recently, it has been validated that oxidative glutamate toxicity toward neurons lacking functional *N*-methyl-D-aspartate receptors can be a component of the excitotoxicity-initiated cell death pathway (15). This form of inducible neuronal death is referred to as oxytosis (18–20). The induction of oxidative stress by glutamate in this model has been demonstrated to be a primary cytotoxic mechanism in C6 glial cells (21–23), PC-12 neuronal cells (24, 25), immature cortical neurons cells (17), and oligodendoglial cells (26).

This work is based on our striking evidence that, in HT4 neuronal cells, nanomolar concentrations of α-tocotrienol, but not α-tocopherol, block glutamate-induced death by suppressing glutamate-induced early activation of c-Src kinase (27). This function of α-tocotrienol was observed to be independent of its antioxidant property (27). Our previous study presented the first evidence showing that, at amounts 4–10-fold lower than the levels of α-tocotrienol detected in human plasma supplemented with the vitamin E molecule (7), α-tocotrienol has potent signal transduction regulatory properties that account for its neuroprotective function. Of importance, this striking property was exhibited by a nutrient known to be safe for human consumption. We sought to characterize the molecular

* This work was supported by NINDS Grant NS42617 from the National Institutes of Health (to C. K. S.). The modeling studies were additionally supported by NIDDK Grant 56631 from the National Institutes of Health (to P. W. S.). The costs of publication of this article were defrayed in part by the payment of page charges. This article must therefore be hereby marked "*advertisement*" in accordance with 18 U.S.C. Section 1734 solely to indicate this fact.

[S] The on-line version of this article (available at http://www.jbc.org) contains Supplemental Video I (*.avi* file of 73 frames collected once every 15 min for 18 h; exported to *.avi* format at 300 ms/frame; total length of 21.9 s; compatible with Microsoft Windows Media Player) and Video II (*.avi* file of 33 frames collected once every 15 min for 18 h; exported to *.avi* format at 300 ms/frame; total length of 9.9 s; compatible with Microsoft Windows Media Player) of Fig. 2, *i–l* and *m–p*, respectively.

‖ To whom correspondence should be addressed: 512 Dorothy M. Davis Heart and Lung Research Inst., The Ohio State University Medical Center, 473 W. 12th Ave., Columbus, OH 43210. Tel.: 614-247-7786; Fax: 614-247-7818; E-mail: sen-1@medctr.osu.edu.

mechanisms responsible for the potent neuroprotective property of trace amounts of tocotrienol. The results from the current line of investigation identified the 12-lipoxygenase (LOX)[1] pathway as being sensitive to tocotrienol. Although a major publication has identified 12-LOX as a critical facilitator of glutamate-induced cell death in HT4 neurons (16), we present the first evidence demonstrating that the glutamate-induced 12-LOX activity is sensitive to nanomolar concentrations of tocotrienol. Additionally, in further support of the key role of 12-LOX in executing glutamate-induced neuronal death, we show that 12-LOX-deficient primary cortical neurons are resistant to glutamate challenge.

EXPERIMENTAL PROCEDURES

Materials

The following materials were obtained from the sources indicated: L-glutamic acid monosodium salt, arachidonic acid, dimethyl sulfoxide, L-buthionine (*S*,*R*)-sulfoximine (BSO), and L-homocysteic acid (Sigma); baicalein (5,6,7-trihydroxyflavone, BL15) (Oxford Biomedical Research, Inc., Oxford, MI); and α-tocotrienol (commercially available as Tocomin™ for human dietary supplementation) (Carotech, Ipoh, Malaysia; BASF, Ludwigshafen, Germany). Dulbecco's modified Eagle's medium, minimal essential medium, fetal calf serum, penicillin, and streptomycin (Invitrogen) and culture dishes (Nunc, Roskilde, Denmark) were used for cell culture.

Cell Culture

Mouse hippocampal HT4 cells (provided by Dr. D. E. Koshland, Jr., University of California, Berkeley, CA) (27) were grown in Dulbecco's modified Eagle's medium supplemented with 10% fetal calf serum, 100 units/ml penicillin, and 100 μg/ml streptomycin at 37 °C in a humidified atmosphere of 95% air and 5% CO_2.

Primary Cortical Neurons—Cells were isolated from the cerebral cortex of rat fetuses (Sprague-Dawley rats, day 17 of gestation) or mouse fetuses (C57BL/6 mice, day 14 of gestation) as described (17). For the 12-LOX knockout studies, neurons were isolated from the fetuses of B6.129S2-Alox15^{tm1Fun} mice (Jackson Laboratory, Bar Harbor, ME). After isolation from the brain, cells were counted and seeded on culture plates at a density of 2–3 × 10^6 cells/35-mm plate (17). Cells were grown in minimal essential medium supplemented with 10% heat-inactivated fetal bovine serum, 40 μM cystine, and antibiotics (100 μg/ml streptomycin, 100 units/ml penicillin, and 0.25 μg/ml amphotericin). Cultures were maintained at 37 °C in 5% CO_2 and 95% air in a humidified incubator. All experiments were carried out 24 h after plating.

Treatment with Neurotoxic Agents—Immediately before experiments, the culture medium was replaced with fresh medium supplemented with serum and antibiotics. Glutamate (10 mM) was added to the medium as an aqueous solution (23, 27, 28). No change in the medium pH was observed in response to the addition of glutamate. Other agents used to induce death in neuronal cells are described in the pertinent figure legends.

Vitamin E Treatment—Stock solutions (10^3 times the working concentration) of α-tocotrienol was prepared in ethanol. The respective controls were treated with an equal volume of ethanol (0.1%, v/v). α-Tocotrienol was added to the culture dishes either 5 min before or after the glutamate treatment as indicated in the figure legends.

Determination of Cell Viability

Viability of HT4 cells was determined using a propidium iodide exclusion assay and a flow cytometer as described by us previously (27, 28). Because primary neuronal cultures tend to aggregate during flow cytometry, the viability of these cells was assessed by measuring lactate dehydrogenase leakage (23) from cells to the medium 24 h after glutamate treatment using an *in vitro* toxicology assay kit from Sigma as described in detail in a previous report (23). In brief, cell viability was determined using the following equation: viability = lactate dehydrogenase activity of cells in monolayer/total lactate dehydrogenase activity (*i.e.* lactate dehydrogenase activity of cells in monolayer + lactate dehydrogenase activity of detached cells + lactate dehydrogenase activity in the cell culture medium).

12-Lipoxygenase Expression

To overexpress 12-LOX in HT4 cells, the cells were transiently transfected with plasmid pcDNA3.1+12-LOX (ResGen, Invitrogen) or pcDNA3.1 using FuGENE 6 (Roche Applied Science) following the instructions of the manufacturer. To assess the level of 12-LOX expression, HT4 cells were harvested 24 h after transfection, and the protein concentrations were determined using BCA protein reagents. Samples (20 μg of protein/lane) were separated on a NuPAGE™ 4–12% BisTris gel (Invitrogen) under reducing conditions, transferred to a polyvinylidene difluoride membrane, and probed with anti-12-LOX polyclonal antiserum (Cayman Chemical Co., Inc., Ann Arbor, MI). To evaluate the loading efficiency, membranes were stripped and reprobed with anti-β-actin antibody (Sigma).

Cytosol Preparation

Cells (1.7 × 10^6) were seeded on 140 × 20-mm plates. After 12–18 h, cells (two plates/sample) were washed with ice-cold phosphate-buffered saline (PBS) and harvested by scraping from the dishes. Samples were spun at 700 × *g* for 5 min at 4 °C. Buffer (400 μl) containing 10 mM HEPES (pH 7.8), 10 mM KCl, 1 mM Na_2EDTA, 2 mM $MgCl_2$, 5% glycerol, 1 mM dithiothreitol, 1 mM phenylmethylsulfonyl fluoride, 5 μg/ml leupeptin, 5 μg/ml aprotinin, and 5 μg/ml antipain was added to the cell pellet. Samples were resuspended and kept on ice for 15 min. After 15 min, 30 μl of 10% Nonidet P-40 was added to each sample, and the samples were vortexed for 30 s. This was followed by centrifugation at 14,000 × *g* for 20 min at 4 °C. The cystolic supernatant was collected and kept at −80 °C. The protein concentrations were determined using BCA protein reagents.

Total Membrane Preparation

Cells (1.7 × 10^6) were seeded on 140 × 20-mm plates. After 12–18 h, cells (five plates/sample) were harvested for total membrane preparation. Total membranes were prepared as described previously (29). After washing with ice-cold PBS, cells were harvested by scraping. Samples were spun at 700 ×*g* for 10 min at 4 °C. Buffer (10 ml) containing 20 mM NaHEPES (pH 7.4), 250 mM sucrose, 2 mM EGTA, 1 mM sodium azide, 100 μM phenylmethylsulfonyl fluoride, and 1 μM protease inhibitor mixture (Sigma) was added to the cell pellet. Samples were homogenized using a motor-driven homogenizer (15 strokes) at 4 °C. Samples were then spun at 760 × *g* for 3 min at 4 °C. After centrifugation, the supernatant was collected and spun at 190,000 × *g* for 1 h at 4 °C. The resulting total membrane pellet was resuspended in the above-mentioned buffer, and samples were stored at −80 °C. The protein concentrations were determined using BCA protein reagents.

12-Lipoxygenase Activity

To investigate whether tocotrienol directly affects the activity of 12-LOX, 10 units of 12-LOX (BIOMOL Research Labs Inc. (Plymouth Meeting, PA) was incubated at room temperature for 15 min with or without tocotrienol as indicated in the figure legends. The reaction mixture contained 50 mM Tris-HCl (pH 7.4) and 1 mM EDTA. After 15 min, the reaction was initiated by the addition of 25 μM [1-^{14}C]arachidonic acid to each sample. Samples were kept at 37 °C for 30 min. The reaction was terminated by the addition of 200 μl of ice-cold stop solution containing diethyl ether, methanol, and 1 M citric acid at a ratio of 30:4:1 (v/v). After mixing, the samples were centrifuged, and the ethereal extracts were spotted on a silica gel thin layer plate. Thin layer chromatography was performed using a solvent system of diethyl ether, petroleum ether, and acetic acid at a ratio of 85:15:0.1 (v/v) for 45–60 min at −20 °C. Distribution of the radioactivity of the substrate and products on the plate was quantified using an imaging analyzer.

Glutathione Assay

GSH was detected using an HPLC coulometric electrode array detector (Coularray Detector Model 5600 with 12 channels, ESA Inc., Chelmsford, MA). Sample preparation and the mobile phase and column used for glutathione assay were as previously described (27). As an improvement to previously reported methods, the current method implemented a coulometric electrode array detector for the detection of glutathione (30). This system uses multiple channels with different redox potentials. Glutathione was detected at channels set at the following potentials: (i) 600 mV, (ii) 700 mV, and (iii) 800 mV. Signals from the channel set at 800 mV were used for quantification (31).

12-Hydroxyeicosatetraenoic Acid (12-HETE) Detection

12-HETE in HT4 cells was detected using an HPLC/UV-based method (32).

[1] The abbreviations used are: LOX, lipoxygenase; BSO, L-buthionine (*S*,*R*)-sulfoximine; BisTris, 2-[bis(2-hydroxyethyl)amino]-2-(hydroxymethyl)propane-1,3-diol; PBS, phosphate-buffered saline; HPLC, high performance liquid chromatography; 12-HETE, 12-hydroxyeicosatetraenoic acid.

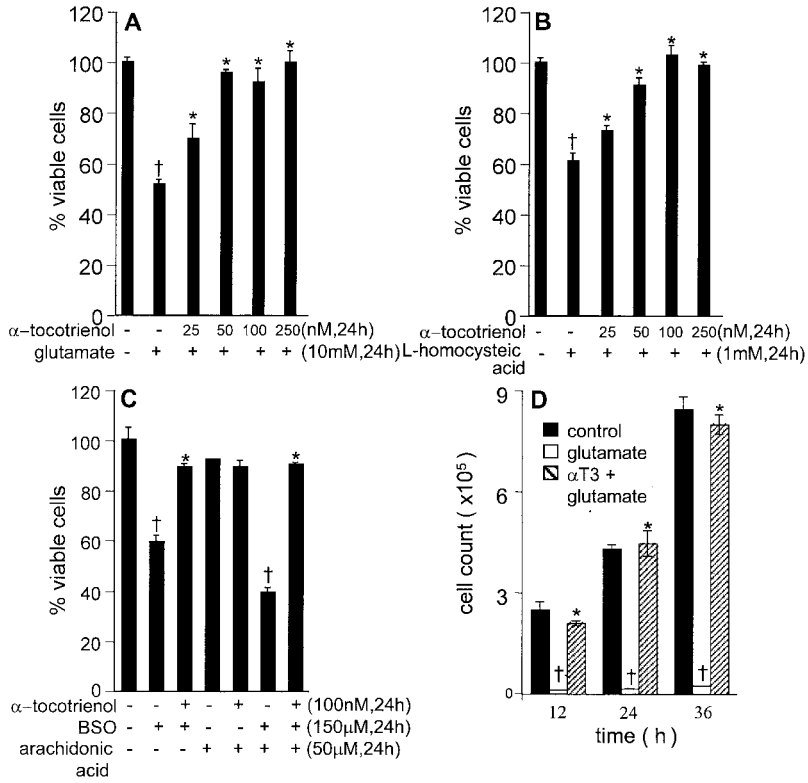

FIG. 1. **Protection against loss of neuronal viability by α-tocotrienol.** Rat immature primary cortical neurons (*A–C*) or HT4 neurons (*D*) were either treated or not with α-tocotrienol as indicated for 5 min and challenged with glutamate (10 mM; *A*), L-homocysteic acid (1 mM; *B*), or BSO (0.15 mM; *C*) for 24 h. Arachidonic acid (0.05 mM; *C*) potentiated BSO-induced cell death. α-Tocotrienol conferred total protection against all of the above neurotoxins. 100 nM α-tocotrienol (α*T3*) not only prevented glutamate-induced toxicity, but allowed glutamate-treated cells to proliferate at a rate comparable to cells not treated with glutamate (*D*). Cells were counted at 12, 24, and 36 h after glutamate challenge. *A*: †, lower compared with the control glutamate-untreated group; *, higher compared with the glutamate-treated group. *B*: †, lower compared with the control L-homocysteic acid-untreated group; *, higher compared with the L-homocysteic acid-treated group. *C*: †, lower compared with the corresponding control; *, higher compared with the corresponding group challenged with toxin(s). *D*: †, lower compared with the corresponding control untreated group; *, higher compared with the corresponding glutamate-treated group. $p < 0.05$.

Immunofluorescence Microscopy

For immunofluorescence microscopy, primary cultures of rat cortical neurons were plated on 35-mm plates precoated with poly-L-lysine. After 24 h, cell were treated with α-tocotrienol or BL15 for 5 min and then challenged with glutamate or exposed to glutamate. After 24 h of glutamate exposure, cells were washed three times with PBS, fixed for 10 min at room temperature in 4% paraformaldehyde, and permeabilized with PBS/T (PBS containing 0.2% Triton X-100) for 20 min at room temperature. Samples were then rinsed three times with PBS/T, and blocking (2% bovine serum albumin in PBS/T) was done for 1 h at room temperature. After blocking, samples were incubated overnight at 4 °C with the primary antibody (anti-neurofilament 200 (diluted 1:100; Sigma) or anti-neuronal class III β-tubulin (diluted 1:500; Covance, Berkeley, CA)). After washing with PBS (three times, 5 min each), the samples were incubated with Alexa Fluor 488-conjugated goat anti-mouse or anti-rabbit secondary antibody (Molecular Probes In., Eugene, OR) for 45 min at room temperature. This was followed by three PBS washes and mounting in aqueous medium. Fluorescent images were collected using a Zeiss Axiovert 200M microscope. Images were acquired using Axiovision Version 3.1.

Live Cell Imaging

For live cell imaging, primary cultures of rat cortical neurons were plated on 35-mm plates precoated with poly-L-lysine. Live cell imaging was performed with untreated cells from 8 to 26 h (18-h duration) of glutamate exposure because that is the time when morphological changes were most prominent. α-Tocotrienol-treated cells were insensitive to glutamate. These cells were imaged from 26 to 34 h (8-h duration) after glutamate treatment and demonstrated a healthy growth pattern. Images were collected once every 15 min using a specialized phase-contrast Zeiss microscope suited for imaging cells growing on routine culture plates. The microscope was fitted with appropriate accessories to maintain the stage at 37 °C and the gas environment comparable to that of the culture incubator. Images were exported to *.avi* video format using Axiovision Version 4.0.

12-Lipoxygenase Model

Homology model construction was carried out using a Silicon Graphics O2 workstation with 300-MHz MIPS® R5000 (OS IRIX Version 6.5). The theoretical model of 12-LOX was built using the Sybyl GeneFold module (Version 6.8, Tripos Associates, St. Louis, MO). This module employs a BLAST search against the RSCB Protein Database[2] to search for possible protein alignments. The module for identifying homologous proteins uses four scoring functions, which include sequence similarity, local interactions, burial similarity, and secondary structure similarity. These properties are reflected in combination as an "alignment score," with a score of 1000 indicating a perfect alignment with regard to all scoring functions. The target sequence for platelet-type 12-LOX was taken from the NCBI Protein Database. A BLAST search indicated 97% sequence identity and an alignment score of 999.9 with soybean 1-LOX (Protein Data Bank code 1YGE) (33), reflecting a similar folding pattern with the target sequence. The structure of 1YGE was used subsequently as a template protein for model building using the "backbone method" option in Sybyl. Molecular mechanics calculations were performed using the Tripos force field with a constant dielectric function (ϵ 2.0) and a non-bonded cutoff distance of 8.0 Å. The final structure was energy-minimized by a energy convergence gradient value of 0.05 kcal/mol after assigning Gasteiger-Hückel charges. The iron atom was then modeled into a theoretical model. Protein geometry was checked using PROCHECK (34) and was compared with the template protein structure 1YGE.

α-Tocotrienol Docking to 12-Lipoxygenase

Ligand binding studies were carried out using Autodock (Version 3.0.5) (35). Autodock is a compilation of three programs: Autotors, Autogrid, and Autodock (36). Autotors facilitates the input of ligand coordinates; Autogrid pre-calculates a three-dimensional grid of interaction energy based on molecular coordinates; and Autodock performs docking simulations using a lamarckian genetic algorithm. The ligand molecule α-tocotrienol, was constructed using the Sybyl Sketch Molecule option, energy-minimized, and assigned MOPAC charges. Docking was then carried out using standard settings and parameters in Autodock. Figures for the theoretical model and the dockings were generated using MOLMOL software (Version 2K.2, molecule analysis and molecule display).

Data Presentation

Data shown as bar graphs are the means ± S.D. Student's *t* test was used to test the significance of the difference between the means. $p < 0.05$ was interpreted as a significant difference between the means.

[2] Available at www.rcsb.org/pdb.

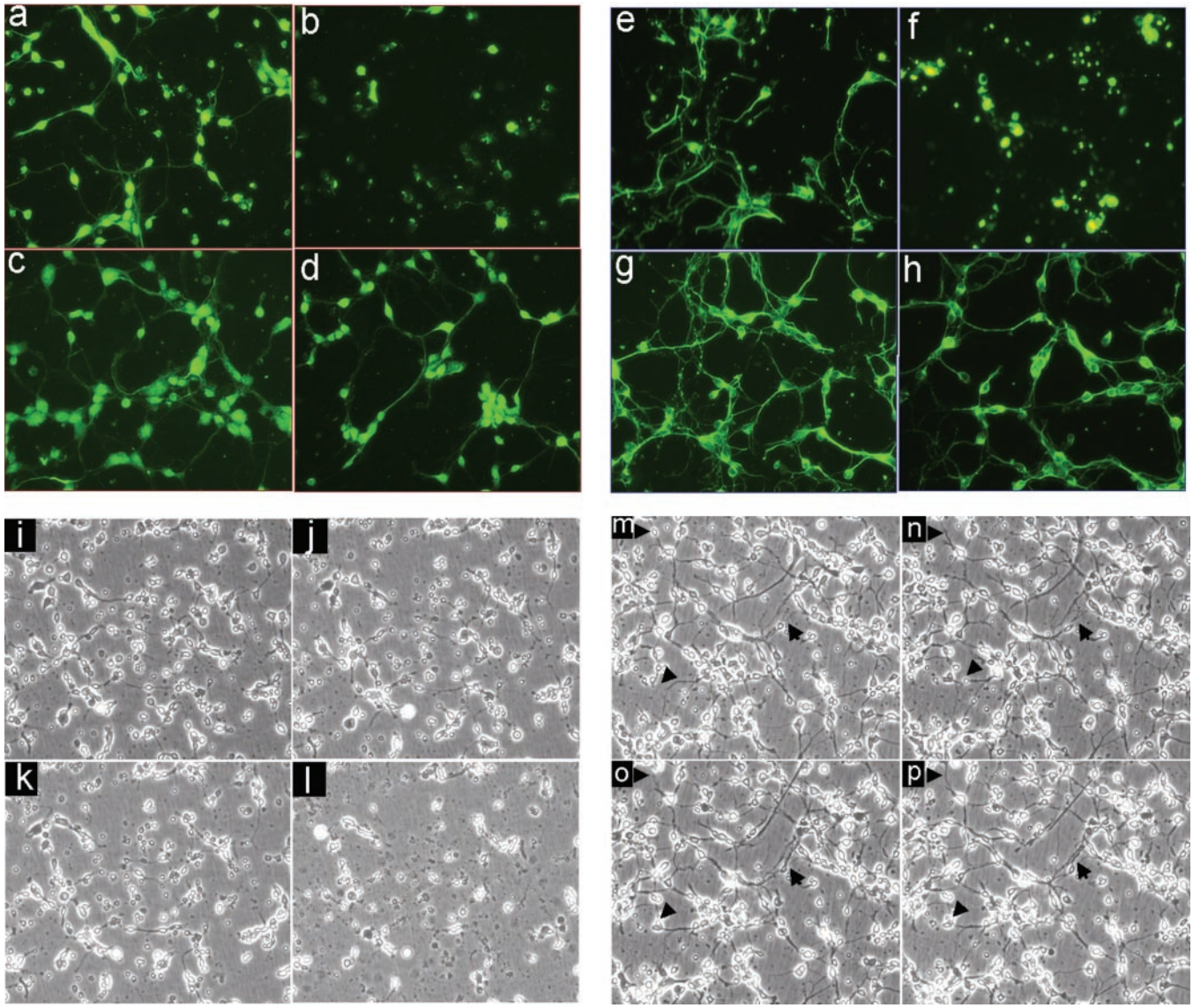

FIG. 2. **Imaging of glutamate-induced degeneration of rat primary cortical neurons and protection by α-tocotrienol and BL15.** After 24 h of seeding, cells were challenged with glutamate. Where indicated, neurons were pretreated with either α-tocotrienol (250 nM) or BL15 (2.5 μM) for 5 min prior to glutamate treatment. *a–d*, neuronal class III β-tubulin staining in the cultured neural network (for phase-contrast microscopy, see *i–p*). After 24 h of glutamate treatment, cells were fixed and stained. *a*, control; *b*, glutamate; *c*, α-tocotrienol + glutamate; *d*, BL15 + glutamate. *e–h*, neurofilament staining in the cultured neural network (for phase-contrast microscopy, see *i–p*). *e*, control; *f*, glutamate; *g*, α-tocotrienol + glutamate; *h*, BL15 + glutamate. *i–p*, live cell imaging of glutamate-treated neurons under standard (not glass coverslip) culture conditions. Phase-contrast images were collected once every 15 min for 18 h from 8 h after glutamate treatment. Frames illustrate time-dependent disintegration of the neural network. *i*, 8 h after glutamate treatment; *j*, 12 h; *k*, 16 h; *l*, 26 h. Glutamate-challenged neurons pretreated with α-tocotrienol (250 nM) resisted degeneration and continued to grow. *m*, 28 h after glutamate treatment; *n*, 30 h; *o*, 32 h; *p*, 34 h. Two *.avi* video micrographs for *i–l* and *m–p* are included in the Supplemental Material. Magnification is ×200.

RESULTS

Previously, we reported the first evidence that nanomolar concentrations of α-tocotrienol protect HT4 neurons from glutamate-induced death independent of its antioxidant property (27). To verify the general relevance of the observed neuroprotective effects of α-tocotrienol, experiments were conducted using primary neuronal cells. We observed that, at nanomolar concentrations, α-tocotrienol clearly protected immature neurons challenged with standard neurotoxins such as glutamate, L-homocysteic acid, and BSO and a combination of BSO and arachidonic acid (Fig. 1, *A–C*). Experiments with HT4 neurons challenged with glutamate revealed that nanomolar levels of α-tocotrienol not only protected against loss of cell viability as reported earlier (27), but preserved the normal growth rate of these cells in culture, suggesting intact cell function (Fig. 1*D*). Challenging primary neurons with glutamate resulted in prominent disruption of the axo-dendritic neural network as evidenced by the staining of β-tubulin and neurofilament and by time-lapse phase-contrast microscopy (Fig. 2, *a–l*). Pretreatment of cells with α-tocotrienol not only prevented glutamate-induced neurodegeneration, but maintained neuronal growth in the face of 10 mM glutamate (Fig. 2, *m–p*). Protection against glutamate-induced structural alterations in the primary neuron was observed by time-lapse phase-contrast microscopy (Fig. 2). We were able to successfully image neurons growing on standard culture plates without having to grow them on glass coverslips. Supplemental Videos I and II demonstrate that, under standard culture conditions, neurons and their axo-dendritic network are fairly motile. This is prominently visible in the micrograph of tocotrienol-treated cells, where glutamate was ineffective in triggering neurotoxicity (Fig. 2, *m–p*). Time-lapse imaging of glutamate-treated control neurons revealed

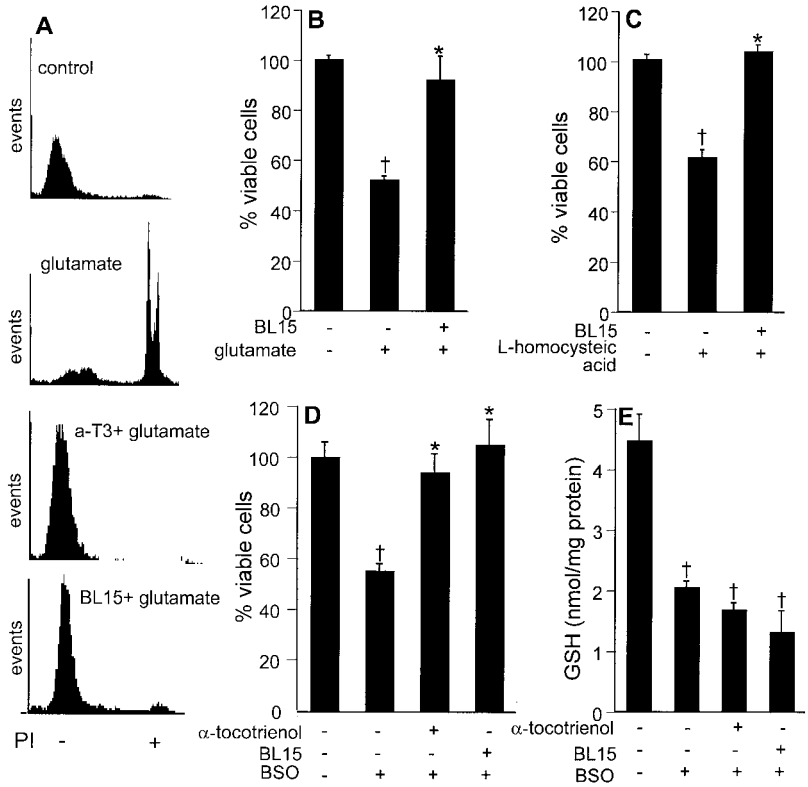

FIG. 3. **Pharmacological inhibition of 12-LOX confers protection against glutamate-induced death of HT4 neurons (*A*) and immature primary cortical neurons (*B–D*).** *A*, HT4 neurons were either treated or not with α-tocotrienol (*α-T3*; 250 nM) or the 12-LOX inhibitor BL15 (2.5 μM) for 5 min and then challenged with glutamate (10 mM). Cell viability was determined using propidium iodide (*PI*) exclusion flow cytometry assay. *PI*−, live; *PI*+, dead. *B–D*, rat immature primary cortical neurons were either treated or not with α-tocotrienol (100 nM) or BL15 (2.5 μM) for 5 min and challenged with glutamate (10 mM; *B*), L-homocysteic acid (1 mM; *C*), or BSO (0.15 mM; *D*) for 24 h. *E*, both α-tocotrienol and BL15 protected neurons against glutamate challenge despite loss of cellular GSH. †, lower compared with the corresponding control untreated group; *, higher compared with the corresponding toxin-treated group. $p < 0.05$.

arrest of cytostructural movements before disruption of the network.

Vitamin E and its analogs are known to be potent inhibitors of 5-LOX (37). This effect is independent of the antioxidant property of vitamin E. Vitamin E is also known to inhibit 15-LOX activity by specifically complexing with the enzyme protein (38). A central role of inducible 12-LOX has been proposed in the execution of glutamate-induced neuronal death (16, 20). Thus, we sought to examine whether the vitamin E α-tocotrienol protects glutamate-induced neurodegeneration by inhibiting 12-LOX activity. First, we tested for the involvement of 12-LOX in the execution of glutamate-induced death in our model. We started by using the 12-LOX-specific inhibitor BL15. Pretreatment of cells with BL15 clearly protected against glutamate-induced death of HT4 cells and primary neurons (Fig. 3, *A* and *B*). In addition, BL15 pretreatment protected primary neurons against toxicity triggered by L-homocysteic acid or BSO (Fig. 3, *C* and *D*). Previously, we reported that nanomolar α-tocotrienol protects against glutamate-induced death of HT4 cells while not sparing glutamate-induced loss of cellular GSH (27). Comparably, BL15-dependent protection against the toxic effects of glutamate was associated with lowered GSH levels in glutamate-treated primary neurons (Fig. 3*E*). Although a few key studies have presented pharmacological evidence supporting that glutamate-induced 12-LOX activation plays a significant role in the execution of neuronal death, conclusive evidence is still missing. We present the first evidence showing that neurons isolated from 12-LOX-deficient mice are resistant to glutamate-induced death (Fig. 4). This striking finding reinforced our interest to test α-tocotrienol as an inhibitor of glutamate-induced 12-LOX activity in neuronal cells. Using an HPLC-based analytical approach, we observed that the by-product of 12-LOX activity, (12*S*)-HETE, was not detected in HT4 cells under basal culture conditions. Glutamate treatment significantly increased cellular (12*S*)-HETE content. However, such an increase was prevented in α-tocotrienol-treated cells (Fig. 5). This line of observation led to the question of whether overexpression of 12-LOX in HT4 cells would sensitize them to glutamate-induced cytotoxicity and whether α-tocotrienol could counter such toxicity. We observed that, in HT4 cells, treatment with glutamate mobilized cytosolic 12-LOX protein to the cell membrane (Fig. 6, *A* and *B*). We were successful in achieving a high level of overexpression in the HT4 neuronal cells (Fig. 6*C*). Such overexpression was associated with increased loss of cell viability by itself (data not shown). As a result, we resorted to an alternative line of investigation to determine whether α-tocotrienol is capable of inhibiting 12-LOX activity. Thin layer chromatographic analysis of 12-LOX activity in the presence of [^{14}C]arachidonic acid revealed that α-tocotrienol dose-dependently inhibited the activity of the pure enzyme (Fig. 6*D*).

The N-terminal domain of lipoxygenases is composed of an eight-stranded antiparallel β-barrel, and its molecular size varies with its genomic origin (mammalian or plant) (39). The description of size and structure for the theoretical model matches the crystal structure of 1YGE. In mammalian species, the C terminus forms the catalytic domain of the enzyme and consists of ~18–22 helices and one antiparallel β-barrel sheet. Two long central helices cross at the active site and include histidines for binding the iron ligand (39). These histidines were observed in our theoretical model at positions 360, 365, and 540 (Fig. 7*A*). The terminal isoleucine plays an important role in maintaining the size of the active-site cavity (40). The cavity for the iron atom can also be observed in the homology model. This is the center for dioxygenation reaction and substrate binding (41). There are 30 solvent cavities that can be observed in the theoretical model, with the highest cavity size of 124 Å^3, which is in the vicinity of the active site. The PROCHECK protein geometry assessment for the theoretical model determined that 85% of the residues fall within the allowed region as compared with 88% for 1YGE. The other residues fall within the generously allowed region. Autodock calculated free binding energies for 10 different docking positions and sorted them in increasing order of binding energy (Fig. 7*D*). The

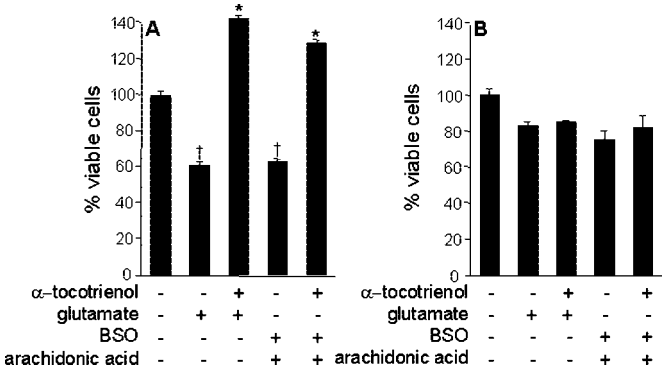

FIG. 4. **Immature primary cortical neurons isolated from 12-LOX knockout mice are resistant to glutamate-induced death.** Murine immature primary cortical neuronal cells (C57BL/6 (*A*) and B6.129S2-Alox15^{tm1Fun} (*B*)) were challenged with glutamate (10 mM) for 24 h. Cell viability was assessed by lactate dehydrogenase assay. Treatment specifications are described in the legend of Fig. 1. α-Tocotrienol was present at 100 nM. †, lower compared with the corresponding control untreated group (also lower compared with the corresponding group in 12-LOX-deficient neurons); *, higher compared with the corresponding toxin-treated group. $p < 0.05$.

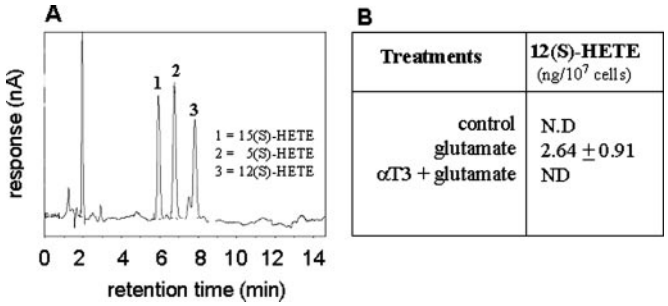

FIG. 5. **Products of 12-LOX activity in glutamate-treated neurons.** *A*, shown is a representative chromatogram for HETE, a key by-product of lipoxygenase activity. *B*, glutamate treatment for 12 h resulted in elevated levels of (12*S*)-HETE, a product of 12-LOX activity, in HT4 neurons. *αT3*, α-tocotrienol; *ND*, not detectable.

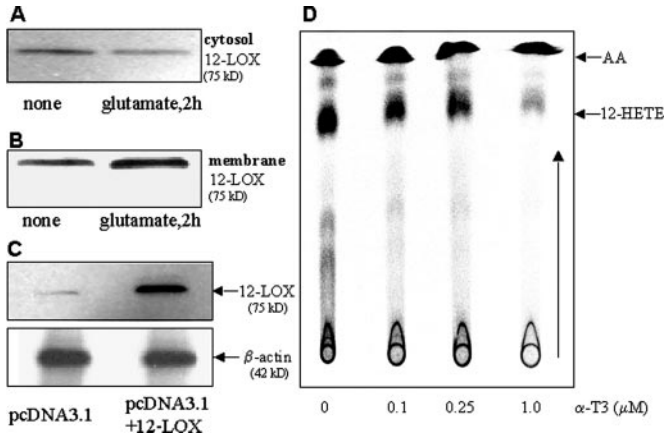

FIG. 6. **12-LOX: overexpression, localization, and sensitivity to α-tocotrienol.** In HT4 cells, glutamate treatment for 2 h resulted in the diminished presence of 12-LOX in the cytosol (*A*) and its increased presence in the membrane (*B*), suggesting mobilization of the enzyme from the cytosol to the membrane. The successful overexpression of 12-LOX in HT4 cells (*C*) and the dose-dependent inhibition of pure 12-LOX activity by α-tocotrienol (*α-T3*; *D*) are shown. Purified 12-LOX (porcine leukocyte; 10 units) was incubated with [^{14}C]arachidonic acid (*AA*; 25 μM) for 30 min at 37 °C. Arachidonic acid and 12-HETE were resolved by thin layer chromatography as described under "Experimental Procedures."

docked energy is calculated from the free energy of binding and internal energy of ligand. The inhibition constant is subsequently correlated to the docked energy. We found that α-tocotrienol is concentrated at the opening of a solvent cavity close to the active site (Fig. 7, *B* and *C*), thereby effectively blocking the entrance of the substrate for this enzyme, arachidonic acid.

DISCUSSION

Vitamin E is essential for normal neurological function (42, 43). One of the major objectives of the study of oxytosis of neurons is to understand the mechanisms underlying stroke-related neurodegeneration (15, 20). We have previously reported that α-tocotrienol represents a potent neuroprotective form of vitamin E that completely prevents oxytosis of HT4 neurons at nanomolar concentrations; we showed that inducible neuronal c-Src kinase is a key target of α-tocotrienol (27). In neurons and astrocytes, c-Src is present at 15–20 times higher levels than in fibroblasts. The specific activity of the c-Src protein from neuronal cultures is 6–12 times higher than that from astrocyte cultures, suggesting a key function of this protein in neurons (44). However, the potential role of c-Src in brain pathophysiology remains unknown. Our results proved that glutamate-induced c-Src activation represents a major checkpoint in oxytosis of HT4 cells (27). A subsequent study confirmed *in vivo* that Src deficiency or blockade of Src activity in mice provides cerebral protection following stroke (45). Our current findings demonstrate that the potent neuroprotective properties of α-tocotrienol are not limited to HT4 cells, but apply to primary cortical neurons as well. GSH is a key survival factor in cells of the nervous system, and lowered intracellular [GSH] is one of the early markers of neurotoxicity induced by a variety of agonists (46, 47). We observed that α-tocotrienol clearly protected primary cortical neurons against a number of GSH-lowering neurotoxins. Of interest, the neurons survived even in the face of GSH loss. These observations lead to the hypothesis that loss of intracellular [GSH] alone is not lethal. Given that pro-GSH agents are known to be neuroprotective in a variety of scenarios (23, 47, 48), it becomes reasonable to hypothesize that glutamate-induced lowering of intracellular [GSH] triggers downstream responses that execute cell death. Indeed, it has been demonstrated that the lowering of neuronal intracellular [GSH] triggers the activation of neuronal 12-LOX, which leads to the production of peroxides, the influx of Ca^{2+}, and ultimately cell death (16). We have reported that specific inhibition of 12-LOX by BL15 protected neurons from glutamate-induced degeneration, although intracellular [GSH] was compromised by 80%. Similar protective effects of BL15 were noted when BSO, a specific inhibitor of GSH synthesis, was used as the agonist. These lines of observation suggest a critical role of 12-LOX in mediating neurodegeneration caused by GSH-lowering agents such as glutamate. Most of the results supporting the contention were, however, derived from studies using pharmacological inhibitors that are likely to have nonspecific effects. Our current results demonstrate that neurons isolated from mice lacking the 12-LOX gene are resistant to glutamate-induced loss of viability. This constitutes a key piece of evidence establishing that 12-LOX indeed represents a critical checkpoint in glutamate-induced neurodegeneration.

Understanding the intracellular regulation of 12-LOX requires knowledge of the distribution of both the enzyme protein and its activity. For example, in human erythroleukemia cells, the membrane fraction contains ~90% of the total cellular 12-LOX activity, whereas only 10% of the 12-LOX activity resides in the cytosol; however, the majority of cellular 12-LOX protein is found in the cytosol (49). Upon activation, 12-LOX has been suggested to translocate to the membrane (49). We

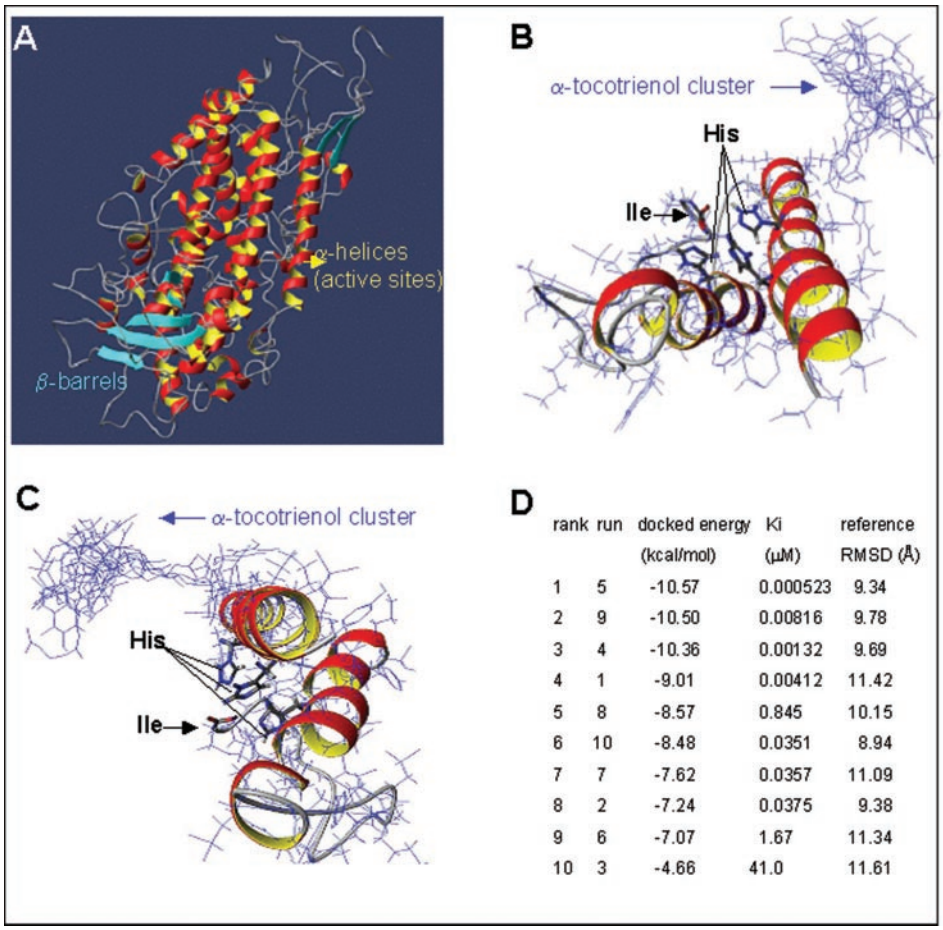

FIG. 7. **Three-dimensional modeling of 12-LOX and α-tocotrienol docking analysis.** *A*, three-dimensional structure of 12-LOX. Homology model construction was carried out using a Silicon Graphics O2 workstation with 300-MHz MIPS R5000 (OS IRIX Version 6.5). The theoretical model of 12-LOX was built using the Sybyl GeneFold module (Version 6.8). *B* and *C*, theoretical model and α-tocotrienol docking (two positions in *B* and *C* are shown with 10 different docking positions). His-360, His-365, His-540, and Ile-663, flanking the iron atom, are visualized in *red*. *D*, Autodock-calculated free binding energies for 10 different docking positions sorted in increasing order of binding energy. *RMSD*, root mean square deviation.

have consistently observed the decreased presence of 12-LOX in the cytosol and its increased presence in the membrane of glutamate-treated cells. For 5-LOX, both catalytic function and translocation of the enzyme from the cytosol to the membrane are known to be regulated by tyrosine kinases (50). Although we have demonstrated that α-tocotrienol specifically modulates tyrosine phosphorylation in glutamate-treated neurons (27), the role of such kinases in the translocation of 12-LOX remains to be tested.

Neurons of the central nervous system are rich in arachidonic acid, (20:4*n*-6 polyunsaturated fatty acid). Lipoxygenases, mainly 5-, 12-, and 15-LOXs, are named for their ability to insert molecular oxygen at the 5-, 12-, or 15-carbon atoms of arachidonic acid, forming a distinct hydroperoxyeicosatetraenoic acid (51). 12-LOX produces (12*S*)-hydroperoxyeicosatetraenoic acid, which is further metabolized into four distinct products: an alcohol ((12*S*)-HETE), a ketone (12-ketoeicosatetraenoic acid), and two epoxy alcohols (hepoxilins A3 and B3). Immunohistochemical studies revealed the occurrence of 12-LOX in neurons: particularly in the hippocampus, striatum, and olivary nucleus as well as in glial and cerebral endothelial cells (52, 53). Using immature cortical neurons and HT4 cells, it has been shown that a decrease in intracellular [GSH] triggers the activation of neuronal 12-LOX, which leads to the production of peroxides, the influx of Ca^{2+}, and ultimately cell death (16, 20). Lipoxygenase sensitivity to vitamin E has been previously reported. α-Tocopherol has been shown to strongly inhibit purified 5-LOX with an IC_{50} of 5 μM. The inhibition is independent of the antioxidant property of tocopherol. Tryptic digestion and peptide mapping of the 5-LOX·tocopherol complex indicated that tocopherol binds strongly to a single peptide (37). Another study reported inhibition of 15-LOX by tocopherol via specific interaction with the enzyme protein (38). Of interest, inhibitors specific for cyclooxygenase or 5-LOX are not effective in protecting neuronal cells against glutamate-induced death, suggesting a specific role of 12-LOX in glutamate-induced death (16). Our studies addressing the effect of α-tocotrienol on pure 12-LOX suggest the possibility that α-tocotrienol directly interacts with the enzyme to suppress arachidonic acid metabolism. *In silico* studies examining possible docking sites of α-tocotrienol on 12-LOX support the presence of an α-tocotrienol-binding solvent cavity close to the active site. It has previously been demonstrated in 15-LOX that the C terminus of arachidonic acid enters this solvent cavity while accessing the catalytic site (40). It is therefore plausible that the binding position of α-tocotrienol prevents access of the natural substrate arachidonic acid to the active site of 12-LOX.

At concentrations well within the physiologically relevant range, α-tocotrienol exhibits potent neuroprotective properties in HT4 and immature primary cortical neurons. Our results confirm a central role of 12-LOX in executing glutamate-induced oxidative toxicity of neurons and offer α-tocotrienol as a promising tool in nutrition-based therapeutics.

REFERENCES

1. Brigelius-Flohe, R., and Traber, M. G. (1999) *FASEB J.* **13,** 1145–1155
2. Traber, M. G., and Sies, H. (1996) *Annu. Rev. Nutr.* **16,** 321–347
3. Traber, M. G., and Packer, L. (1995) *Am. J. Clin. Nutr.* **62,** 1501S–1509S
4. Serbinova, E. A., and Packer, L. (1994) *Methods Enzymol.* **234,** 354–366
5. Suarna, C., Hood, R. L., Dean, R. T., and Stocker, R. (1993) *Biochim. Biophys. Acta* **1166,** 163–170
6. Tomeo, A. C., Geller, M., Watkins, T. R., Gapor, A., and Bierenbaum, M. L. (1995) *Lipids* **30,** 1179–1183
7. O'Byrne, D., Grundy, S., Packer, L., Devaraj, S., Baldenius, K., Hoppe, P. P., Kraemer, K., Jialal, I., and Traber, M. G. (2000) *Free Radic. Biol. Med.* **29,** 834–845
8. Azzi, A., Boscoboinik, D., Marilley, D., Ozer, N. K., Stauble, B., and Tasinato, A. (1995) *Am. J. Clin. Nutr.* **62,** 1337S–1346S
9. Boscoboinik, D. O., Chatelain, E., Bartoli, G. M., Stauble, B., and Azzi, A. (1994) *Biochim. Biophys. Acta* **1224,** 418–426
10. Pearce, B. C., Parker, R. A., Deason, M. E., Dischino, D. D., Gillespie, E., Qureshi, A. A., Volk, K., and Wright, J. J. (1994) *J. Med. Chem.* **37,** 526–541
11. Pearce, B. C., Parker, R. A., Deason, M. E., Qureshi, A. A., and Wright, J. J. (1992) *J. Med. Chem.* **35,** 3595–3606
12. Suzuki, Y. J., Tsuchiya, M., Wassall, S. R., Choo, Y. M., Govil, G., Kagan, V. E., and Packer, L. (1993) *Biochemistry* **32,** 10692–10699
13. Choi, D. W. (1990) *Cerebrovasc. Brain Metab. Rev.* **2,** 105–147
14. Tan, S., Sagara, Y., Liu, Y., Maher, P., and Schubert, D. (1998) *J. Cell Biol.* **141,** 1423–1432
15. Schubert, D., and Piasecki, D. (2001) *J. Neurosci.* **21,** 7455–7462
16. Li, Y., Maher, P., and Schubert, D. (1997) *Neuron* **19,** 453–463
17. Murphy, T. H., Schnaar, R. L., and Coyle, J. T. (1990) *FASEB J.* **4,** 1624–1633
18. Sagara, Y., Ishige, K., Tsai, C., and Maher, P. (2002) *J. Biol. Chem.* **277,** 36204–36215
19. Dargusch, R., and Schubert, D. (2002) *J. Neurochem.* **81,** 1394–1400
20. Tan, S., Schubert, D., and Maher, P. (2001) *Curr. Top. Med. Chem.* **1,** 497–506
21. Kato, S., Negishi, K., Mawatari, K., and Kuo, C. H. (1992) *Neuroscience* **48,** 903–914
22. Han, D., Handelman, G., Marcocci, L., Sen, C. K., Roy, S., Kobuchi, H., Tritschler, H. J., Flohe, L., and Packer, L. (1997) *Biofactors* **6,** 321–338
23. Han, D., Sen, C. K., Roy, S., Kobayashi, M. S., Tritschler, H. J., and Packer, L. (1997) *Am. J. Physiol.* **273,** R1771–R1778
24. Froissard, P., Monrocq, H., and Duval, D. (1997) *Eur. J. Pharmacol.* **326,** 93–99
25. Pereira, C. M., and Oliveira, C. R. (1997) *Free Radic. Biol. Med.* **23,** 637–647
26. Oka, A., Belliveau, M. J., Rosenberg, P. A., and Volpe, J. J. (1993) *J. Neurosci.* **13,** 1441–1453
27. Sen, C. K., Khanna, S., Roy, S., and Packer, L. (2000) *J. Biol. Chem.* **275,** 13049–13055
28. Tirosh, O., Sen, C. K., Roy, S., and Packer, L. (2000) *Neuroscience* **97,** 531–541
29. Bashan, N., Burdett, E., Hundal, H. S., and Klip, A. (1992) *Am. J. Physiol.* **262,** C682–C690
30. Roy, S., Venojarvi, M., Khanna, S., and Sen, C. K. (2002) *Methods Enzymol.* **352,** 326–332
31. Sen, C. K., Khanna, S., Babior, B. M., Hunt, T. K., Ellison, E. C., and Roy, S. (2002) *J. Biol. Chem.* **277,** 33284–33290
32. Eberhard, J., Jepsen, S., Albers, H. K., and Acil, Y. (2000) *Anal. Biochem.* **280,** 258–263
33. Bernstein, F. C., Koetzle, T. F., Williams, G. J., Meyer, E. F., Jr., Brice, M. D., Rodgers, J. R., Kennard, O., Shimanouchi, T., and Tasumi, M. (1977) *Eur. J. Biochem.* **80,** 319–324
34. Laskowski, R., MacArthur, M. W., Moss, D. S., and Thornton, J. M. (1993) *J. Appl. Crystallogr.* **26,** 283–291
35. Morris, G. M., Goodsell, D. S., Halliday, R. S., Huey, R., Hart, W. E., Belew, R. K., and Olson, A. J. (2001) *Autodock Reference Manual*, Version 3.0.5, The Scripps Research Institute, La Jolla, CA
36. Goodsell, D. S., Morris, G. M., and Olson, A. J. (1996) *J. Mol. Recognit.* **9,** 1–5
37. Reddanna, P., Rao, M. K., and Reddy, C. C. (1985) *FEBS Lett.* **193,** 39–43
38. Grossman, S., and Waksman, E. G. (1984) *Int. J. Biochem.* **16,** 281–289
39. Minor, W., Steczko, J., Stec, B., Otwinowski, Z., Bolin, J. T., Walter, R., and Axelrod, B. (1996) *Biochemistry* **35,** 10687–10701
40. Borngraber, S., Browner, M., Gillmor, S., Gerth, C., Anton, M., Fletterick, R., and Kuhn, H. (1999) *J. Biol. Chem.* **274,** 37345–37350
41. Gillmor, S. A., Villasenor, A., Fletterick, R., Sigal, E., and Browner, M. F. (1997) *Nat. Struct. Biol.* **4,** 1003–1009
42. Muller, D. P., and Goss-Sampson, M. A. (1989) *Ann. N. Y. Acad. Sci.* **570,** 146–155
43. Muller, D. P., and Goss-Sampson, M. A. (1990) *Crit. Rev. Neurobiol.* **5,** 239–263
44. Brugge, J. S., Cotton, P. C., Queral, A. E., Barrett, J. N., Nonner, D., and Keane, R. W. (1985) *Nature* **316,** 554–557
45. Paul, R., Zhang, Z. G., Eliceiri, B. P., Jiang, Q., Boccia, A. D., Zhang, R. L., Chopp, M., and Cheresh, D. A. (2001) *Nat. Med.* **7,** 222–227
46. Dringen, R., Gutterer, J. M., and Hirrlinger, J. (2000) *Eur. J. Biochem.* **267,** 4912–4916
47. Bains, J. S., and Shaw, C. A. (1997) *Brain Res.* **25,** 335–358
48. Schulz, J. B., Lindenau, J., Seyfried, J., and Dichgans, J. (2000) *Eur. J. Biochem.* **267,** 4904–4911
49. Hagmann, W., Kagawa, D., Renaud, C., and Honn, K. V. (1993) *Prostaglandins* **46,** 471–477
50. Lepley, R. A., Muskardin, D. T., and Fitzpatrick, F. A. (1996) *J. Biol. Chem.* **271,** 6179–6184
51. Yamamoto, S. (1992) *Biochim. Biophys. Acta* **1128,** 117–131
52. Nishiyama, M., Watanabe, T., Ueda, N., Tsukamoto, H., and Watanabe, K. (1993) *J. Histochem. Cytochem.* **41,** 111–117
53. Nishiyama, M., Okamoto, H., Watanabe, T., Hori, T., Hada, T., Ueda, N., Yamamoto, S., Tsukamoto, H., Watanabe, K., and Kirino, T. (1992) *J. Neurochem.* **58,** 1395–1400

Molecular Basis of Vitamin E Action: TOCOTRIENOL MODULATES 12-LIPOXYGENASE, A KEY MEDIATOR OF GLUTAMATE-INDUCED NEURODEGENERATION

Savita Khanna, Sashwati Roy, Hoon Ryu, Praveen Bahadduri, Peter W. Swaan, Rajiv R. Ratan and Chandan K. Sen

J. Biol. Chem. 2003, 278:43508-43515.
doi: 10.1074/jbc.M307075200 originally published online August 13, 2003
